Influence of temperature and charge effects on thermophoresis of polystyrene beads

Olga Syshchyk^{1,2}, Dzmitry Afanasenkau¹, Zilin Wang¹, Hartmut Kriegs¹, Johan Buitenhuis¹, and Simone Wiegand^{1,3}

- ¹ ICS-3 Soft Condensed Matter, Forschungszentrum Juelich GmbH, D-52428 Juelich, Germany
- ² Institute of High Technologies, Taras Shevchenko National University of Kyiv, 01601 Kyiv, Ukraine
- ³ Chemistry Department Physical Chemistry, University Cologne, D-50939 Cologne, Germany

Received: date / Revised version: date

Abstract. We study the thermodiffusion behavior of spherical polystyrene beads with a diameter of 25 nm by infra-red thermal diffusion Forced Rayleigh Scattering (IR-TDFRS). Similar beads were used to investigate the radial dependence of the Soret coefficient by different authors. While Duhr and Braun [P. Natl. Acad. Sci. USA, 104 (2007) 9346] observed a quadratic radial dependence Braibanti et al. [Phys. Rev. Lett., 100 (2008) 108303] found a linear radial dependence of the Soret coefficient. We demonstrated that special care needs to be taken to obtain reliable thermophoretic data, because the measurements are very sensitive to surface properties. The colloidal particles were characterized by transmission electron microscopy and dynamic light scattering (DLS) experiments were performed. We carried out systematic thermophoretic measurements as a function of temperature, buffer and surfactant concentration. The temperature dependence was analyzed using an empirical formula. To describe the Debye length dependence we used a theoretical model by Dhont. The resulting surface charge density is in agreement with previous literature results. Finally, we analyze the dependence of the Soret coefficient on the concentration of the anionic surfactant sodium dodecyl sulfate (SDS), applying an empirical thermodynamic approach accounting for chemical contributions.

PACS. 42.40.-i discribing text of that key -66.10.cd discribing text of that key -66.30.Xj discribing text of that key -65.20.-w discribing text of that key -66.10.cg discribing text of that key -82.70.Dd discribing text of that key

1 Introduction

Thermodiffusion (or Thermophoresis or Ludwig-Soret effect) describes the mass diffusion in a mixture of at least two components due to a temperature gradient. It competes with Fickian diffusion creating a concentration gradient along the temperature gradient. In a binary mixture the mass flux \boldsymbol{i} of one component can be described by [1]

$$\mathbf{j} = -D\nabla c - c(1-c)D_{\mathrm{T}}\nabla T, \qquad (1)$$

with concentration, c, temperature, T, diffusion coefficient D and the thermal diffusion coefficient $D_{\rm T}$. The first term in equation 1 describes mass transport due to a concentration gradient while the second one introduces the flux due to the temperature gradient. For a time independent temperature gradient, a steady state is reached when the mass flux contributions due the Fickian- and thermodiffusion cancel each other out. The ratio of the resulting concentration gradient and the applied temperature gradient is characterized by the Soret coefficient $S_T = D_{\rm T}/D$. In the past years a couple of reviews appeared summarizing the experimental and theoretical results for liquid mixtures, polymer solutions and colloidal dispersions [2, 3, 4, 5].

Since its discovery in the middle of the nineteenth century by Ludwig [6] and systematic studies by Soret [7] the effect is used in applications in different areas such as isotope separation [8] and characterization of polymers and colloids with the thermal field flow fractionation [9]. In the recent years the effect gained a lot of interest in the so called microscale thermophoresis, where it is used to characterize biomolecular reactions in solutions [10]. Despite of a long history of investigations a microscopic theory which can explain the effect in liquids still does not exist. The phenomenon depends on a large number of parameters such as mass, size and surface charge of the particle, the hydration shell and collective effects between different particles [2]. In contrast to simulations it is often not possible to vary the parameters in the experiment independently from each other, so that cross effects occur, which leads to a rather complex picture.

The temperature dependence of $S_{\rm T}$ of a solute molecule at low concentration dissolved in water can often be described by an empirical formula suggested by Iacopini et al. [11]

$$S_{\rm T}(T) = S_{\rm T}^{\infty} \left[1 - \exp\left(\frac{T_{inv} - T}{T_0}\right) \right]$$
 (2)

with fitting parameters $S_{\rm T}^{\infty}$, T_{inv} and T_0 . Systems such as ethanol/water [12], DMSO/water [13] and crown ether in water [14] deviate from this empirical law at low concentrations. While other systems like formamide/water show deviations for larger concentrations of the solute, if interactions between different solute molecules start to play a role [15]. At the present state of knowledge, we can state that Eq.2 holds only if the solute molecules are well connected to water by hydrogen bonds and no microheterogeneous structures or cages are formed.

The thermophoretic behavior of charged colloidal particles has been investigated experimentally [16, 17, 18, 19] and theoretically [20, 21, 20, 22]. Some of the theoretical approaches consider thermoelectric effects generated by the cloud of counter-ions [21, 22], while others consider the thermophoretic force on the charged colloidal particle due to the presence of its double layer [20, 20]. Sehnem et al. could describe the temperature dependence of the Soret coefficient of a ferro fluid by using a combination of both approaches. The thermophoretic behavior of charged Ludox particles [16] and the bare fd-virus [23, 17] was measured as a function of the Debye screening length by adjusting the buffer concentration. For both systems the Soret coefficient increased with increasing Debye length and could be described by a theoretical model, which was originally derived for spherical particles by Dhont [20, 24]. The theoretical approach was later extended to long and thin charged rods and agreed nicely with the experimental results [17] and gave also the surface charge density, which is in agreement with electrophoretic measurements. In conclusion we can state that if the electric double layer contributions dominate the thermophoretic behavior compared to other short range interactions a convincing theoretical concept exists.

As thermophoresis depends on many physical and chemical properties [25] one should have a stable model system, which allows the variation of one of the parameters like size or surface properties while keeping the others constant. Spherical monodisperse polymeric colloidal particles such as polystyrene (PS) beads have been used as a model system for many studies of thermophoresis. They are considered to be simple and well characterized. PS particles are available with different diameters and surface groups and for optical observation with a microscope they can be fluorescently labeled, which does not changes the surface properties, as the fluorophore molecules can be placed inside the beads. Several groups used PS beads to study thermophoresis of colloids. Duhr and Braun [26], Braibanti et al. [27] and Putnam et al. [28] studied the Soret coefficient dependence on the particle size. It was also used by Zhao et al. to study collective effects on thermophoresis of colloids [29]. It turns out that the thermophoresis is influenced by changes of the surface properties of the particles, which vary for different producers and even from batch to batch. Additionally, the presence

of stabilizing additives such as surfactants or preservatives which can be often found in commercial products, change the surface properties of the particles. On the other hand, washing the particles and placing them in a standard solvent such as deionized water or buffer may lead to changes of stability and particle aggregation.

All these factors influence the thermophoretic properties and cause a wide spread of data points as shown in figure 1, which displays the Soret coefficient of polystyrene beads (PS) measured by different authors as a function of the bead diameter [26, 27, 28, 29]. The majority of the groups studied carboxyl modified PS beads. For the particles with the smaller diameters (d < 50nm) often negative Soret coefficients have been observed [27, 28]. Also in this work we observed for the particles used without further treatment a negative Soret coefficient. Only for the particles which we dialyzed against water we observed a positive Soret coefficient as it was also the case in the work of Duhr and Braun [30]. Only for the polystyrene bead with the lowest radius Braibanti et al. [27] find a negative $S_{\rm T}$, while all other $S_{\rm T}$ -values for larger radii are positive and larger than those obtained by Duhr and Braun [26]. Both groups dialyzed there solutions against a buffer solution so

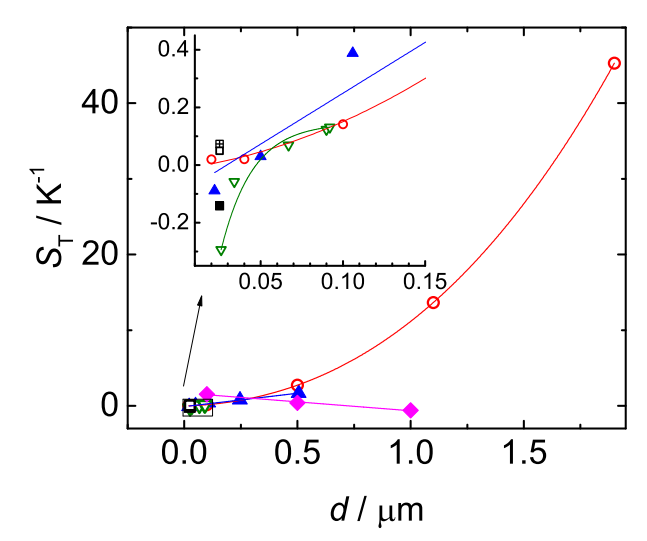


Fig. 1. Literature data of the Soret coefficient S_T of PS beads in aqueous solution at room temperature (red open circles) carboxyl modified, c < 0.003%, 1mM Tris, pH=7.6, $T = 22^{\circ}\mathrm{C}$ [26]; (filled blue triangle) - carboxyl modified, c = 0.35%, 1mM Tris, pH=7.8, $T = 25^{\circ}$ C [27]; (green open triangle down) - carboxyl modified, c = 1.5 - 2.1%, deionized water, T = 30°C [28]; (filled magenta diamond) - sulfate modified, c = 0.02 - 2%, deionized water, $T = 30^{\circ} \text{C}$ [29]; in this work we performed measurements of carboxyl modified beads at $T = 25^{\circ}$ C under different conditions: for solutions dialyzed against water c =0.97% at pH=3.5 (black square with cross) and at pH=8 (black open square) and for a solution with the stabilizing surfactants from the supplier at c = 1.0%, pH=3.2 (filled black square). The inset shows a magnification of the area marked by the bounding box. The lines are linear, second order polynomial or exponential fits. Note that the lines in the inset represent fits over all data points shown in the full graph.

that differences in the behavior should not be influenced by the stabilizing surfactant, but additionally concentration effects and the attachment of a fluorescent label can play a role. The measured concentrations differ by more than a factor of 100. Therefore the thermophoretic properties of the PS particles need to be characterized in a systematic way and the experimental conditions need to be specified carefully.

In this paper we study thermophoretic properties of PS nanoparticles using the IR-TDFRS method. We put special effort in the characterization of the particle properties to find possible reasons which explain the different literature results. Additionally, we use transmission electron microscopy (TEM) to investigate the size distribution of particles and dynamic light scattering (DLS) to characterize diffusive properties and to check for possible agglomeration. We study the influence of the buffer ionic strength and show that the theory by Dhont [20, 24] for the thermophoresis of charged spheres can be used to describe the results. Additionally, we investigate the influence of the surfactant sodium dodecyl sulfate (SDS) on the thermophoresis of the beads and describe the surfactant concentration dependence of the Soret coefficient $S_{\rm T}$, as a combination of the Dhont model for charged spheres and an empirical thermodynamic expression describing the chemical contributions.

2 Experimental Details

2.1 Sample and preparation

The fluorescent polystyrene beads with a diameter of 25 nm (Fluoro-Max Dyed Green Aqueous Fluorescent Particles) were purchased from Thermo Scientific, Inc (Catalog No. G25). The particles are suspended in aqueous solution with a weight concentration of 1.0%. According to the information provided by the supplier [31] the suspension contains a trace amount of ethylenediaminete-traacetic acid (EDTA) and an anionic surfactant similar to SDS as a preservative to inhibit aggregation and promote stability. The surface of the beads are modified with carboxyl-groups, which leads to a negative surface charge.

The polystyrene beads were dialysed against a buffer solution or deionized water to remove additives, which can influence the thermophoretic properties of the system (cf. Section 3). The dialysis tubes (FLOAT-A-LYZER G2, CE, 50KD, 1ML) were purchased from Spectrum Labs, Inc. The dialysis tube with the particle dispersion was kept in a stirred solution for several days. The reservoir solution was changed 3 times. To tune the ionic strength we chose Tris(hydroxymethyl)aminomethane (Tris) buffer with a concentration range of 1.9-46 mM. The solutions in deionized water were put in an ultrasonic bath for 15-20 minutes to dissolve aggregates.

The concentration of particles after dialysis was determined by absorption spectrometry (Varian Cary 50 Bio UV-Visible Spectrophotometer) using a calibration curve. For the low concentrations we performed a dilution series and the concentration was obtained from the absorption

at a wavelength of 466 nm, while at higher concentrations we took a defined volume and determined the mass of the solid content after evaporation of the solvent.

For the systematic studies of the influence of the surface properties, we added the ionic surfactant sodium dodecyl sulfate (Sigma Aldrich, purity $\geq 99\%$), after we had dialyzed the particles (c=0.5%) against di-ionized water. We varied the concentration of sodium dodecyl sulfate (SDS) between $0.3\mu\mathrm{M}$ and $15\mathrm{mM}$, whereas the critical micelle concentration lies around $8.2\mathrm{mM}$ [32].

2.2 Experimental methods

The size distribution of the fluorescent polystyrene beads was measured by transmission electron microscopy (TEM). We used a Libra 120 (Carl Zeiss NTS GmbH) with an accelerating voltage of 120kV. A drop of the suspension with an approximate volume of $15\mu L$ with a concentration of $c=0.5 {\rm wt\%}$ was placed on a carbon coated copper grid on a filter paper to suck away the excess of the drop. The specimen was dried in an oven at 334K for at least 30 minutes before recording the TEM image.

Additionally, we performed dynamic light scattering (DLS) measurements using an ALV-5000 multi-tau digital correlator (Langen, Germany). We performed measurements in a concentration range between 0.1-0.5wt% of the beads at room temperature (293K) in a TRIS/HCl buffer with HCl approximately half the TRIS concentration typically resulting in a pH of 8.2. We used four TRIS concentrations of 2.88mM, 5.1mM, 10mM and 46.2mM. All samples were filtered prior to the measurements with a $0.2\mu m$ filter (Whatman Anotop 10) and the concentration was determined after filtering the sample. Note that the dispersion of the PS beads in deionized water without the addition of a surfactant became instable and the obtained distribution functions were bimodal, while the addition of the buffer increased the stability of the solutions.

Our IR-TDFRS set-up is described elsewhere [23]. The IR-TDFRS is optimized for aqueous systems as it utilizes an infrared laser to create a temperature gradient due to absorption of the light energy by water [33]. This method works nicely for molecules, polymers and small particles. For larger particles the measurement time becomes longer due to the slower diffusion, so that the stability of the measurement can become an issue. The particles with a diameter of 25 nm can be measured reliably. Approximately 2 mL of the prepared solutions were filtered through a 0.2 μ m filter (Whatman Anotop 10) before filling into an optical quartz cell (Hellma) with an optical path length of 0.2 mm. At least two measurements with different cells and freshly prepared samples were performed for each system.

3 Results

3.1 Particle characterization

We characterized the particles with respect to size with TEM, which was used for direct particle visualization (see

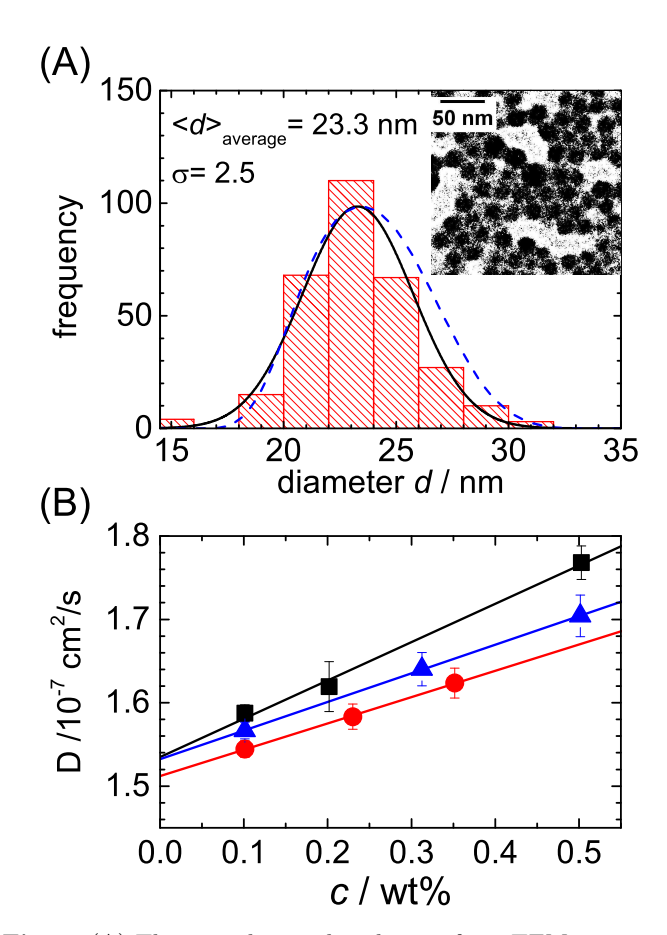


Fig. 2. (A) The particle-size distribution from TEM imaging. The blue dashed line is a typical distribution determined from DLS measurements by a CONTIN analysis. (inset) A typical TEM image of the particles. (B) Diffusion coefficients D measured for different buffer concentrations 5.1mM (black square), 10mM (blue triangle up) and 46.2mM (red bullet) as a function of the mass concentration of the PS beads. All measurements were performed at $T=20^{\circ}\mathrm{C}$ and pH=8.2.

Fig. 2(A), inset). By analyzing the images the diameter distribution of the particles was obtained. Using a Gaussian distribution we obtained a mean diameter at 23.3 nm with a standard deviation of $\sigma = 2.5$ nm (see Fig. 2(A)).

Additionally we performed DLS experiments of the particles in different solutions. Note that at higher concentrations and for long-range interactions the diffusion coefficient is influenced by collective effects and deviates from the Stokes-Einstein diffusion coefficient D_0 , which corresponds to the hydrodynamic radius R_h using the relation $R_h = kT/(6\pi\eta D_0)$. The addition of the salt (in our case TRIS) to a charged system reduces the repulsive interactions between the particles. Therefore, an increase of the ionic strength leads to a smaller collective diffusion coefficient D, provided temperature and concentration are kept constant. Figure 2(B) shows this effect as a function of the PS bead concentration. For very low concentrations the curves should approach D_0 , which implies that the dif-

ferences between the diffusion coefficients measured at the different buffer concentrations become smaller.

The observation that the collective diffusion slows down with increasing TRIS content might be counter intuitive, because, due to the larger Debye length of the macroions at low TRIS, their volume is larger than in the case of high TRIS, so that they should diffuse faster in the later case. This holds for the long-time self-diffusion coefficient [34], but not for the collective diffusion coefficient, which can be expressed as $D(q) = D_0 \cdot H(q)/S(q)$ within the Smoluchowski dynamics of overdamped particle motion [35]. The diffusion coefficient of an isolated particle is denoted as D_0 , the hydrodynamic function as H(q) and the static structure factor as S(q). Any q-dependence of H(q)is an indicator for the influence of hydrodynamic interactions, while without hydrodynamic interaction $H(q) \equiv 1$. In the long wave length limit S(q) can be approximated by $S(0) \equiv \lim_{n \to \infty} S(q) = \rho_0 k_B T \chi_T$ and is proportional to the isothermal osmotic compressibility χ_T , which describes the deviations from an ideal solution and increases with increasing salt content, so that the collective diffusion becomes smaller [35]. The same observation has been made for apoferritin by Gapinski et al. [36]. Only for very high volume fractions the situation might be inversed since then the hydrodynamic interactions dominate the behavior [37].

Extrapolating the collective diffusion coefficient D linearly to zero concentration we obtain $D_0 = (1.53 \pm 0.02) \cdot 10^{-7} \mathrm{cm}^2 \mathrm{s}^{-1}$, which results in a hydrodynamic radius of $R_h = 14.1 \pm 0.2 \mathrm{nm}$ using the Stokes-Einstein equation. D_0 is the mean of the solutions with the three higher buffer concentrations. This D_0 -value obtained by DLS is slightly higher than the radius determined by the TEM measurements, which is expected because the TEM measurements give a number average, while DLS gives a z-average of the inverse hydrodynamic radius, $\left\langle R_h^{-1} \right\rangle_z$ [38].

3.2 Temperature dependence

We investigated the thermophoretic properties of the polystyrene beads in the solution as received from the supplier (pH=3.2), in deionized water (pH=3.4) and in a 10mM TRIS buffer (pH=8.2) solution. The temperature dependences of the Soret coefficient $(S_{\rm T})$ for all three solutions is shown in figure 3. As can be seen the beads in the native solution from the supplier show thermophilic behavior $(S_{\rm T}$ is negative), the behavior becomes thermophobic $(S_{\rm T}$ is positive) if the beads are placed in deionized water or in a buffer solution. The $S_{\rm T}$ -values for particles in deionized water and in buffer are close to each other and show a similar temperature dependence.

The Soret coefficient of the diluted solutions of polystyrene beads can be described by Eq.2 for all three solutions. The corresponding fitting parameters are listed in table 1 and show for the solution with pH=8.2 large uncertainties and in the case of the solution with pH=3.4 one parameter had to be fixed. For comparison we show in Fig. 3 also the linear fit as dashed lines. In all three cases the linear fit is sufficient to describe the temperature dependence of the Soret coefficient in the investigated temperature range.

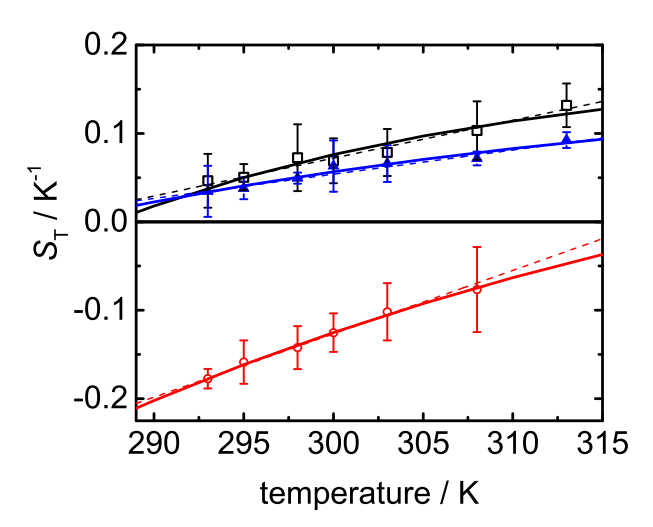


Fig. 3. $S_{\rm T}$ of the PS beads as a function of temperature for the solution as received from the supplier with a concentration of 1% by weight (pH=3.2) (red open circles), dialyzed against deionized water (pH=3.4) (black open squares) and in a 10mM TRIS buffer solution at pH=8.2 (blue solid triangles). The solid and dashed lines refer to a fit according to Eq.2 and a linear fit, respectively.

Table 1. Fitting parameters of PS beads according to Eq.2 for the solid curves displayed in Fig. 3.

	pH=3.2			pH=3.4			pH=8.2		
				(deionized)			(TRIS buffer)		
S_{T}^{∞}	0.19	±	0.04	0.18	±	0.01	0.17	\pm	0.14
T_{inv}	325.6	\pm	5.3	288	\pm	1	285	\pm	4
T_0	46.2	\pm	6.8		23		37	\pm	49

3.3 Influence of the ionic strength

We measured $S_{\rm T}$, $D_{\rm T}$ and D as a function of the Deby length (see Fig. 4) at pH = 8.2. The Soret coefficient decreases with increasing the Debye length, while the opposite trend was observed in previous experiments with charged Ludox particles [16] and charged fd-virus [17]. Simultaneously, we observe for the same weight fraction around 1% that the collective diffusion coefficient D increases by a factor 10 in the investigated Debye length range, while the thermal diffusion coefficient $D_{\rm T}$ increases only by a factor 2.5. As already discussed in Section 3.1 the strong increase of D is caused by decreasing osmotic compressibility with decreasing salt content [36]. Reducing the weight fraction to c = 0.35% we observe no dependence of D (see Fig. 4 open blue squares) on the Debye length. The large difference in the diffusion coefficient measured for the two different concentration can be resolved, if we plot the mass diffusion coefficient as a function of the effective volume fraction (Fig.4). The measured mass diffusion coefficient at the two concentrations of 0.35% and 0.98% falls on a master curve, as they should. Finally we can state that the collective diffusion coefficient depends more on

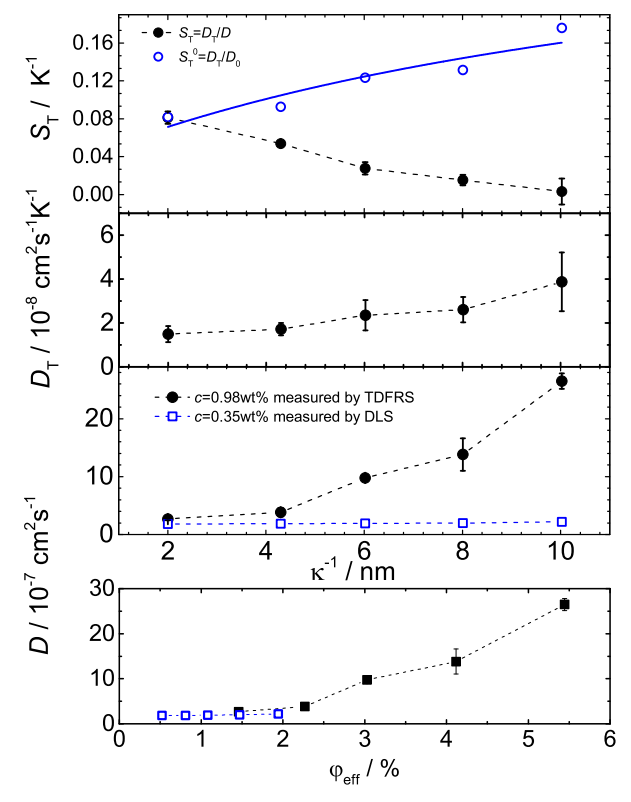


Fig. 4. Soret coefficient $S_{\rm T}$ and thermal diffusion coefficient $D_{\rm T}$ as a function of the Debye length κ^{-1} measured at $T=25^{\circ}{\rm C}$. The open blue circles represent $S_{\rm T}^0=D_{\rm T}/D_0$ using the Stokes-Einstein diffusion coefficient for the diluted solution with $c=0.35{\rm wt}\%$ (blue open squares). The collective diffusion coefficient D is additionally shown in dependence of the effective volume fraction, $\varphi_{\rm eff}=\varphi\left(\left(R+\kappa^{-1}\right)/R\right)^3$. The blue solid line corresponds to a fit according to Eq. 4 and the dashed lines connect the points. The particle concentrations for the IR-TDFRS and DLS were 0.98 ± 0.01 and 0.35 ± 0.01 wt%, respectively.

interactions between the colloidal beads than the thermal diffusion coefficient $D_{\rm T}$.

The Debye length dependence of $S_{\rm T}$ of spherical colloids can be described by an expression originally derived by Dhont (Eq. (45) in Ref.24), where the Debye length κ^{-1} is given by

$$\kappa^{-1} = \sqrt{\frac{1}{8\pi l_B N_A I}} \tag{3}$$

with Avogadro's number N_A and $l_B = \beta e^2/(4\pi\epsilon)$ is the Bjerrum length (0.71 nm for water at room temperature). Since the acid dissociation constant pK_a of Tris is 8.2 as what we use in the paper, the ionic strength I is half the value of the total molar concentration of Tris buffer. Therefore we can easily tune the Debye length κ^{-1} by adjusting the concentration of the Tris buffer. In contrast to the original capacitor model [26] this expression works for thin and thick double layers. In the theoretical approach, $S_{\rm T}$ of a charged colloidal sphere with radius R can be

expressed by

$$S_{\mathrm{T}}^{\mathrm{charge}} = \frac{1}{T} \left\{ 1 + \frac{1}{4} \left(\frac{4\pi l_B^2 \sigma}{e} \right)^2 \frac{1}{(1 + \kappa R)^2} \frac{\kappa R^4}{l_B^3} \right.$$

$$\times \left[1 - \frac{d \ln \epsilon}{d \ln T} \left(1 + \frac{2}{\kappa R} \right) \right] \right\} + A(T) ,$$

$$(4)$$

where $\beta = 1/(k_BT)$ with k_B is the Boltzmann constant, ϵ is the dielectric constant of water at ambient temperature, e is the elementary charge, σ is the surface charge density, R is the radius of the particle, $1/\kappa$ is the Debye length, A(T) is the additive contribution from the solvation layer and the core material of the colloid. The factor $d\ln\epsilon/d\ln T$ is equal to -1.34 for water at room temperature.

Note, that the thermal diffusion coefficient is obtained from the measured Soret coefficient and the measured collective mass diffusion coefficient. In a prior study it was found that the thermal diffusion coefficient is insensitive to concentration at a given Debye length [17]. Assuming the same behavior for the here studied particles, the variation of the thermal diffusion coefficient is due to the change of the Debye length. The single-particle Soret coefficient $S_{\rm T}^0$ calculated according to Eq.4 is thus obtained by dividing the experimental thermal diffusion coefficient obtained as described above, by the mass diffusion coefficient at infinite dilution. We use diffusion coefficient measured for the diluted solution with c = 0.35wt% (see blue circles in Fig. 4). Indeed $S_{\rm T}^0$ can be described by Eq. 4 with a surface charge density of $\sigma = 2.5 \cdot 10^4 e/\mu m^2$, which is reasonable compared to published literature values. The magnitude of this value is five times larger than the surface charge density $\sigma = 0.45 \cdot 10^4 e/\mu m^2$ for negatively charged PS particles published by Ning et al. [16] and 20-50 times smaller compared to the surface charge density measured for positively charged PS particles at pH=9.5 and pH=5 [39]. Note that the surface charge density depends strongly on the pH [40]. Behrens and Grier determined at pH=8.2 a $8.5 \mathrm{\ times\ higher\ surface\ charge\ density\ assuming\ carboxyl}$ group density of 0.25 nm⁻². The lower value found could be a consequence of different number of surface groups or of counter ion condensation.

3.4 Influence of surfactant

The presence of the surfactant plays a crucial role in the thermophoresis of PS beads. The addition of a surfactant has been used to create a better standardized particle-solvent interface [27] and to prevent agglomeration. The DLS measurements of the particles dispersed in deionized water indicated the presence of aggregates in the absence of a surfactant. In order to study the influence of the surfactant on the thermophoresis we performed a systematic study adding different concentrations of sodium dodecyl sulfate (SDS) in water. SDS is an anionic surfactant with a dodecyl-chain attached to a sulfate group. The contour length of the molecule is in the order of 2 nm and according to the information by the distributor of the studied PS beads SDS is similar to the surfactant, which is used

for stabilization of the particles. The pH of the solutions was around 3.4 ± 0.2 .

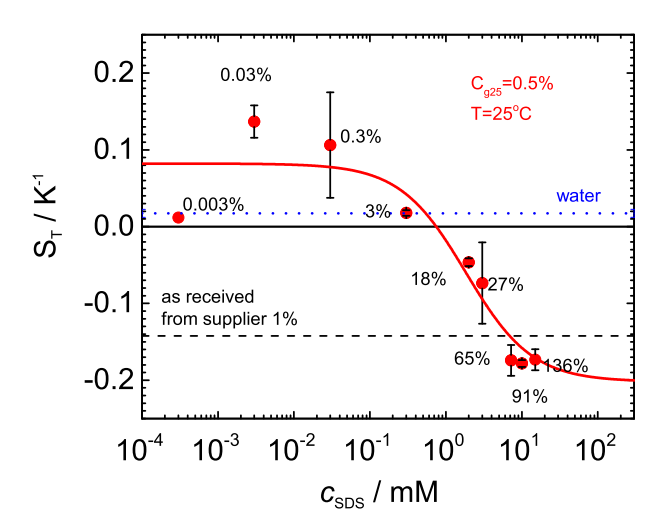


Fig. 5. The $S_{\rm T}$ of the PS beads in an aqueous surfactant solution in dependence of the surfactant concentration. The particle concentration is $c=0.5\pm0.01~\%$ by weight and the measurements where performed at $T=25^{\circ}{\rm C}$. The numbers near to each point are rough estimates of particle surface covered by the surfactant molecules, assuming that the area occupied by the surfactant molecule is determined by the cross section of the head group. The solid line is a fit according to Eq. 9 with the fitting parameters listed in Table 2. Further details are given in the text.

The $S_{\rm T}$ as a function of the surfactant concentration is shown in fig. 5. Except for the lowest surfactant concentration and pure water $S_{\rm T}$ decreases with increasing surfactant and reaches a plateau at a surfactant concentration around 7.2mM.

There is no obvious reason for the low $S_{\rm T}$ -values of pure water and the very low surfactant concentration of 0.0003mM SDS. In aqueous systems one often finds a more thermophobic behavior (increase of $S_{\rm T}$) when solute molecules with a strong tendency to form hydrogen bonds are added [41]. One explanation might be that at this very low concentration the surfactant molecules prefer the horizontal alignment (see Fig. 6) and increase the hydrophobicity of the colloidal particles.

The experimental values at the high surfactant concentrations agree almost with the $S_{\rm T}$ -value obtained for the unwashed particles ($c=1{\rm wt\%}$) from the supplier. The small deviation of the order of 20% can be explained by the unknown surfactant, the addition of EDTA and the two times higher concentration. We assume that a plateau is reached, when the surface of the PS-beads is fully covered with surfactant molecules. Based on the observations by Jeon et al. [42] that the surface groups of a colloidal particle determine its thermophoretic behavior, we assume that the negative Soret coefficient of the colloidal particles fully covered with SDS molecules should be related to thermophoretic behavior of SDS. Comparing with litera-

ture results SDS shows only a negative Soret coefficient in the presence of sodium hydroxide (NaOH), while SDS has a positive Soret coefficient in pure water and in the presence of sodium chloride (NaCl) [43]. Therefore we assume that the COO⁻ group of the COOH-surface groups act in a similar way as NaOH and lead to a negative Soret coefficient.

In order to estimate at which surfactant concentration the surface of the beads is fully covered we consider two scenarios sketched in Figure 6. Typically one assumes that the molecules are perpendicular to the interface (see 6(B) left), but recent vibrational sum frequency scattering studies by de Aguiar et al. [44] indicate that the SDS molecules are parallel to a oil/water interface (6(B) right). In the first scenario the cross section of the head group, while in the second case the area along the alkyl chain needs to be calculated. Using the molecular volumes of the chemical groups [45] we estimate the diameter of the headgroup of SDS and the diameter of the alkyl chain to $d \approx 0.5$ nm. Assuming a coverage due to vertical adsorption of the surfactant molecules (see Fig. 6(B) left) by using the cross section of the head group we estimate that a concentration of 11mM SDS is sufficient to cover all PS beads at c = 0.5wt% corresponding to approximately 1μ M. In our experiment the Soret coefficient saturates already at a slightly lower SDS concentration of 7mM. Note that the actual maximal coverage might be lower, because the steric hindrance and repulsive interactions have not been considered in our coarse estimate. If we assume that SDS adsorbs horizontally on the PS beads, we expect due to the larger contact area in the order of 1.1nm² for the same PS bead concentration a full coverage already at a molar SDS concentration of 1.8mM. If we take the saturation of the Soret coefficient as an indication for full coverage the vertical alignment of the SDS molecules is more compatible with our results. It would be interesting to validate this observation by sum frequency scattering experiments.

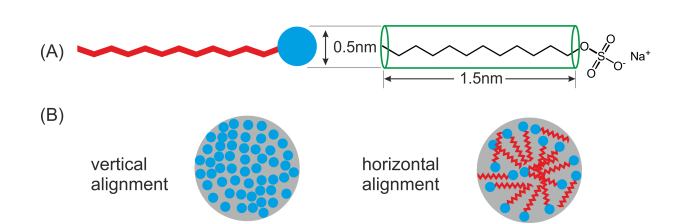


Fig. 6. (A) Geometrical representation and chemical structure of SDS. (B) Illustration of the alignment of the SDS surfactant molecules at the interface of the PS beads: In the vertical alignment the hydrophilic head groups form the interface to water, while the horizontal alignment leads to a more hydrophobic surface due to the alkyl side chain of SDS (this illustration is not true to scale.)

With increasing pH the surface of the carboxylated PS beads becomes more negative. According to Behrens and Grier the surface charge of the carboxylated PS-beads at pH=3.4 \pm 0.2 is negative in the order of σ^{COOH^-} =

 $(-0.9 \pm 0.3) \text{mC/m}^2$ [40]. Adding the ionic surfactant SDS we will increase the total negative charge of the colloidal particles σ :

$$\sigma = \sigma^{\text{COOH}^-} + \sigma^{\text{SDS}} (c_{\text{SDS}}) \tag{5}$$

with

$$\sigma^{\rm SDS}\left(c_{\rm SDS}\right) = \frac{c_{\rm SDS}}{c_p} \cdot \frac{e}{4\pi R^2},\tag{6}$$

where c_p and $c_{\rm SDS}$ denote the molar concentration of the particles and SDS molecules, respectively. As we change the $c_{\rm SDS}$ over three orders of magnitudes also σ varies by three order of magnitude. At the same time the higher ionic strength results due to screening in a shorter Debye length κ^{-1} which can be estimated by

$$\kappa = \sqrt{4\pi N_A l_B (c_{\text{SDS}} + c_{H_3O})}. (7)$$

Note that $c_{\rm SDS}$ is equal to the concentration of the sodium ions c_{Na} , which contributes to the Debye length, while we assume that a 12-carbon tail attached to a sulfate group adsorbs on the bead. The two largest surfactant concentrations of 10 and 15mM are above the critical micelle concentration (cmc) 8.2 mM [46], but the excess part of SDS not bound to the beads is still below the cmc so that we do not expect the formation of micelles. We consider here also the mobile positive H₃O⁺-ions, which can be estimated by the pH-value. Assuming that $S_{\rm T}$ is determined by charge effects and can be described by Eq. 4 and Eq. 6 we expect a quadratic increase of $S_{\rm T}$ with $c_{\rm SDS}$, which is in contradiction with the decay of $S_{\rm T}$ as a function of $c_{\rm SDS}$. Note that this theoretical approach is only valid, if the Debye Hückel approximation and the linearization of the Poisson Boltzmann equation are applicable. At higher SDS concentrations ion condensation and screening effects need to be considered, which require a new theoretical concept, that is beyond the scope of this paper. Therefore we limit the analysis to a heuristic approach describing the chemical contributions.

Unfortunately there is so far no microscopic theory to describe the chemical contribution to $S_{\rm T}$ due to adsorption of the anionic surfactant at the surface of the beads. Often thermodynamic approaches using a heat of transfer concept are applied [47, 48] to describe the chemical contribution to $S_{\rm T}$. In this framework the Soret coefficient of a binary mixture can be expressed by

$$\alpha_{\rm T} = S_{\rm T}^{\rm chem} \cdot T = \frac{a_1 Q_2^* - a_2 Q_1^*}{a \cdot x_1 \left(\frac{\partial \mu_1}{\partial x_1}\right)_{T,p}} \tag{8}$$

whereas Q_2^* , Q_1^* are the heats of transport of component 1 and 2, a_1 , a_2 are the partial molar properties corresponding to the system of coordinates selected. The value of a is an average, determined as $a = a_1 \cdot x_1 + a_2 \cdot x_2$, with the molar fractions x_1 and x_2 . In contrast to organic mixtures where this heat of transfer concept has been successfully used to describe Soret coefficient of binary mixtures [49] for our system the thermophoretic properties such as the activity coefficients are not known. The derivative of the chemical potential for non-ideal solutions can

be expressed as $(\partial \mu_1/\partial x_1)_{T,p} = RT \cdot (\Delta_x + (1/x_1))$ with $\Delta_x = (\partial \ln{(\gamma_1)}/\partial x_1)$. For low concentrations the molar fraction can be approximated by $x_1 = (M_2/M_1) \cdot c_1$. Inserting in Eq. 8 leads after some algebra, where we neglect the cubic and quadratic order terms to the following general form for the chemical contribution to the Soret coefficient S_T^{chem} :

$$S_{\rm T}^{\rm chem} = \frac{c_{\rm SDS} - Q}{\gamma_A + c_{\rm SDS} \cdot \gamma_B} \tag{9}$$

with the adjustable parameters Q, γ_A and γ_B

$$Q = \frac{M_1}{M_2} \cdot \frac{Q_1^*}{Q_{12}}$$

$$\gamma_A = \frac{M_1 \cdot RT^2}{M_2 Q_{12}}$$

$$\gamma_B = (\Delta_x - 2) \cdot \frac{RT^2}{Q_{12}}$$

$$Q_{12} = \left(\frac{\gamma_1}{\gamma_2} Q_2^* + Q_1^*\right)$$

Table 2. Fitting parameters of the solid line displayed in Fig.5 according to Eq. 9 to describe the dependence of the Soret coefficient as a function of the added surfactant concentration.

Parameter	pH=3.4 (deionized)					
Q	0.7	±	0.3			
γ_A	-8.9	\pm	4.1			
γ_B	-4.9	\pm	0.8			

Note that we use $c_{\rm SDS}$ as concentration c_1 . Using 9 we can describe the experimentally determined Soret coefficient as a function of the SDS concentration $c_{\rm SDS}$ (see Fig. 5).

4 Conclusion

In this work we measure thermophoretic properties of polystyrene nanobeads, which are shown to depend strongly on the solvent conditions. The Soret coefficient changes its sign when transferring the particles from their native solution, which contains traces of a detergent and a preservative, into deionized water or buffer solution. This shows a strong dependence on the surface properties. The detergent is probably adsorbed on the particle and modifies the surface charge and hydrophobic properties of the beads. The Debye length dependence of the Soret coefficient $S_{\rm T}$ could be described by the Dhont model resulting in a reasonable value for the surface charge density.

Additionally, we investigated the influence of the added ionic surfactant SDS on the thermophoretic behavior of the beads. It turned out that the thermophoretic behavior is strongly influenced by the changes of the chemical surface of the particles. We used an empirical model to describe the experimentally determined Soret coefficient, which is based on a general thermodynamic expression using the heat of transfer concept. We found a reasonable description of the experimental data, but so far there is no microscopic model to describe the thermophoretic changes due to adsorption of the anionic surfactant.

We conclude that especially the chemical interface of the particles is often difficult to control. Additionally, the interface effects have a strong influence on the thermophoretic data and are responsible for the large spread of experimental data found in the literature. Charge as well as surfactant molecules tend to attach to interfaces. In the case of microfluidic devices also the dimensions of the small cell geometry might influence the results. Coming back to Fig. 1 it should be noted that the cell of Zhao et al. [29] is an all-metal cell, which might release ions with time, so that this leads to the decay of the Soret coefficient with increasing diameter, which has not been observed in any of the other studies. Therefore, all instruments should be validated as it has been done in the Fontainebleau benchmark test [50].

The authors warmly acknowledge useful discussion with Marisol Ripoll, Jan Dhont and Doreen Niether. We thank Silvia DeSio and Yi Liu for their help with the DLS measurements. Part of the experimental data presented was obtained with financial support from the European Commission under the Seventh Framework Program by means of the grant agreement for the Integrated Infrastructure Initiative No. 262348 European Soft Matter Infrastructure (ESMI) which is gratefully acknowledged.

References

- S.R. de Groot and P. Mazur. Non-Equilibrium Thermodynamics. Dover, New York, 1984.
- 2. S. Wiegand. Thermal diffusion in liquid mixtures and polymer solutions. *J. Phys.: Condens. Matter*, 16:R357–R379, 2004.
- 3. R. Piazza and A. Parola. Thermophoresis in colloidal suspensions. *J. Phys-Condens. Mat.*, 20:153102, 2008.
- 4. A. Würger. Thermal non-equilibrium transport in colloids. *Reports on Progress in Physics*, 73:126601, 2010.
- W. Köhler and K. I. Morozov. The soret effect in liquid mixtures - a review. J. Non-Equil. Thermody., 2016.
- 6. C. Ludwig. Diffusion zwischen ungleich erwärmten Orten gleich zusammengesetzter Lösungen. Sitz. ber. Math.-Naturw. Clas. Kais. Akad. Wiss., 20:539, 1856.
- 7. C. Soret. Sur l'etat d'équilibre que prend au point de vue de sa concentration une dissolution saaline primitivement homogéne dont deux parties sont portées a des températures différentes. Arch. Geneve, 3:48–64, 1879.
- 8. K. Clusius and G Dickel. Zur trennung der chlorisotope. *Naturwissenschaften*, 27:148–149, 1939.
- 9. H. Cölfen and M. Antonietti. Field-Flow Fractionation Techniques for Polymer and Colloid Analysis,

- volume 150 of Advances in Polymer Science, pages 67–187. Springer-Verlag Berlin Heidelberg, 2000.
- M. Jerabek-Willemsen, T. André, W. Wanner, H.M. Roth, S. Duhr, P. Baaske, and D. Breitsprecher. Microscale thermophoresis: Interaction analysis and beyond. J. Mol. Struct., pages 101–113, 2014.
- 11. S. Iacopini, R. Rusconi, and R. Piazza. The "macro-molecular tourist": Universal temperature dependence of thermal diffusion in aqueous colloidal suspensions. *Eur. Phys. J. E*, 19:59–67, 2006.
- 12. P. Kolodner, H. Williams, and C. Moe. Optical measurement of the Soret coefficient of ethanol water solutions. *J. Chem. Phys.*, 88:6512–6524, 1988.
- P. Polyakov and S. Wiegand. Systematic study of the thermal diffusion in associated mixtures. *J. Chem. Phys.*, 128:034505, 2008.
- K. Maeda, N. Shinyashiki, S. Yagihara, S. Wiegand, and R. Kita. Ludwig-Soret effect of aqueous solutions of ethylene glycol oligomers, crown ethers, and glycerol: temperature, molecular weight, and hydrogen bond effect. J. Chem. Phys., 143:124504, 2015.
- Doreen Niether, Dzmitry Afanasenkau, Jan K. G. Dhont, and Simone Wiegand. Accumulation of formamide in hydrothermal pores to form prebiotic nucleobases. *Proceedings of the National Academy of Sciences*, 113:4272–4277, 2016.
- H. Ning, J. K. G. Dhont, and S. Wiegand. Thermaldiffusive behavior of a dilute solution of charged colloids. *Langmuir*, 24:2426–2432, 2008.
- Z. Wang, H. Kriegs, J. Buitenhuis, J. K. G. Dhont, and S. Wiegand. Thermophoresis of charged colloidal rods. Soft Matter, 9:8697–8704, 2013.
- A. L. Sehnem, R. Aquino, A. F. C. Campos, F. A. Tourinho, J. Depeyrot, and A. M. F. Neto. Thermodiffusion in positively charged magnetic colloids: Influence of the particle diameter. *Physical Review E*, 89, 2014.
- A. L. Sehnem, A. M. F. Neto, R. Aquino, A. F. C. Campos, F. A. Tourinho, and J. Depeyrot. Temperature dependence of the soret coefficient of ionic colloids. *Physical Review E*, 92, 2015.
- 20. J. K. G. Dhont and W. J. Briels. Single-particle thermal diffusion of charged colloids: Double-layer theory in a temperature gradient. *Eur. Phys. J. E*, 25:61–76, 2008.
- 21. A. Würger. Transport in charged colloids driven by thermoelectricity. *Phys. Rev. Lett.*, 101:108302–1–108302–4, 2008.
- A. Majee and A. Würger. Collective thermoelectrophoresis of charged colloids. *Phys. Rev. E*, 83, 2011.
- 23. P. Blanco, H. Kriegs, M. P. Lettinga, P. Holmqvist, and S. Wiegand. Thermal diffusion of a stiff rod-like mutant y21m fd-virus. *Biomacromolecules*, 12:1602–9, 2011.
- 24. J. K. G. Dhont, S. Wiegand, S. Duhr, and D. Braun. Thermodiffusion of charged colloids: Single-particle diffusion. *Langmuir*, 23:1674–1683, 2007.
- 25. S. Wiegand. Introduction to Thermal Gradient Related Effects, pages F4.1–F4.24. Forschungszentrum

- Jülich, Jülich, 2015.
- 26. S. Duhr and D. Braun. Why molecules move along a temperature gradient? *P. Natl. Acad. Sci. USA*, 103:19678–19682, 2006.
- 27. M. Braibanti, D. Vigolo, and R. Piazza. Does thermophoretic mobility depend on particle size? *Phys. Rev. Lett.*, 100:108303–1–108303–4, 2008.
- 28. S. A. Putnam, D. G. Cahill, and G. C. L. Wong. Temperature dependence of thermodiffusion in aqueous suspensions of charged nanoparticles. *Langmuir*, 23:9221–9228, 2007.
- 29. Y. G. Zhao, C. L. Zhao, J. H. He, Y. Zhou, and C. Yang. Collective effects on thermophoresis of colloids: A microfluidic study within the framework of dlvo theory. *Soft Matter*, 9:7726–7734, 2013.
- 30. S. Duhr and D. Braun. Thermophoretic depletion follows boltzmann distribution. *Phys. Rev. Lett.*, 96:168301–1–168301–4, 2006.
- 31. B. Richards. Answer of the technical support of Thermo Fisher Scientific, 2014.
- 32. P. H. Elworthy and K. J. Mysels. Surface tension of sodium dodecylsulfate solutions and phase separation model of micelle formation. *J. Colloid Interface Sci.*, 21:331–347, 1966.
- 33. S. Wiegand, H. Ning, and H. Kriegs. Thermal diffusion forced rayleigh scattering setup optimized for aqueous mixtures. *J. Phys. Chem. B*, 111:14169–14174, 2007.
- M. G. McPhie and G. Nägele. Long-time self-diffusion of charged colloidal particles: Electrokinetic and hydrodynamic interaction effects. *J. Chem. Phys.*, 127:034906, 2007.
- 35. G. Nägele. The physics of colloidal soft matter, volume 14. Institute of Fundamental Technological Research, Polish academy of Science, Warsaw, 2004.
- J. Gapinski, A. Wilk, A. Patkowski, W. Häussler, A. J. Banchio, R. Pecora, and G. Nägele. Diffusion and microstructural properties of solutions of charged nanosized proteins: Experiment versus theory. *J. Chem. Phys.*, 123:054708, 2005.
- 37. M. P. Lettinga, J. K. G. Dhont, Z. Zhang, S. Messlinger, and G. Gompper. Hydrodynamic interactions in rod suspensions with orientational ordering. *Soft Matter*, 6:4556–4562, 2010.
- 38. S. Wiegand and W. Köhler. *Determination of Molecular Weights and Their Distributions*, volume 53, chapter 6, pages 205–251. Elsevier, Amsterdam, 2008.
- 39. A. F. Barbero, R. M. Garcia, M. A. C. Vilchez, and R. Hidalgoalvarez. Effect of surface-charge density on the electrosurface properties of positively charged polystyrene beads. *Colloids Surf.*, A, 92:121–126, 1994.
- 40. S. H. Behrens and D. G. Grier. The charge of glass and silica surfaces. *J. Chem. Phys.*, 115:6716–6721, 2001.
- 41. R. Sugaya, B. A. Wolf, and R. Kita. Thermal diffusion of dextran in aqueous solutions in the absence and the presence of urea. *Biomacromolecules*, 7:435–440, 2006.

- S. J. Jeon, M. E. Schimpf, and A. Nyborg. Compositional effects in the retention of colloids by thermal field-flow fractionation. *Anal. Chem.*, 69:3442–3450, 1997.
- 43. D. Vigolo, S. Buzzaccaro, and R. Piazza. Thermophoresis and thermoelectricity in surfactant solutions. *Langmuir*, 26:7792–7801, 2010.
- 44. H. B. de Aguiar, M. L. Strader, A. G. F. de Beer, and S. Roke. Surface structure of sodium dodecyl sulfate surfactant and oil at the oil-in-water droplet liquid/liquid interface: A manifestation of a nonequilibrium surface state. J. Phys. Chem. B, 115:2970–2978, 2011.
- 45. H. Durchschlag and P. Zipper. Calculation of the partial volume of organic compounds and polymers. *Ultracentrifugation*, 94:20–39, 1994.
- T.J. Bruno and P.D.N. Svoronos. Surface active chemicals (surfactants). In CRC Handbook of Chemistry and Physics. CRC Press/Taylor & Francis, Internet version 2017.
- 47. K. G. Denbigh. *The Thermodynamics of the Steady State*. Methuen's Monographs on Chemical Subjects. Methuen, London, 1951.
- 48. M. G. Gonzalez-Bagnoli, A. A. Shapiro, and E. H. Stenby. Evaluation of the thermodynamic models for the thermal diffusion factor. *Philos. Mag.*, 83:2171–2183, 2003.
- S. Hartmann, G. Wittko, W. Köhler, K. I. Morozov, K. Albers, and G. Sadowski. Thermophobicity of liquids: Heats of transport in mixtures as pure component properties. *Phys. Rev. Lett.*, 109:065901–1– 065901–4, 2012.
- J. K. Platten, M. M. Bou-Ali, P. Costeseque, J. F. Dutrieux, W. Köhler, C. Leppla, S. Wiegand, and G. Wittko. Benchmark values for the soret, thermal diffusion and diffusion coefficients of three binary organic liquid mixtures. *Philos. Mag.*, 83:1965–1971, 2003.